Hypermorphic *SERK1* Mutations Function via a *SOBIR1* Pathway to Activate Floral Abscission Signaling

Isaiah Taylor,[a,b,c,d] John Baer,[a,b,e] Ryan Calcutt,[a,b,f] and John C. Walker[a,b,1,2]

[a]Division of Biological Sciences, University of Missouri, Columbia, Missouri 65211
[b]Interdisciplinary Plant Group, University of Missouri, Columbia, Missouri 65211
[c]Department of Statistics, University of Missouri, Columbia, Missouri 65211
[d]Department of Biology and Howard Hughes Medical Institute, Duke University, Durham, North Carolina 27708
[e]Department of Medicine, Washington University, St. Louis, Missouri 63130
[f]Biology Department, Washington University, St. Louis, Missouri 63130

ORCID ID: 0000-0002-2050-1641 (J.C.W.).

In Arabidopsis (*Arabidopsis thaliana*), the abscission of floral organs is regulated by two related receptor-like protein kinases, HAESA (HAE) and HAESA-LIKE2 (HSL2). In complex with members of the SOMATIC EMBRYOGENESIS RECEPTOR-LIKE KINASE (SERK) family of coreceptor protein kinases, HAE and HSL2 are activated when bound by INFLORESCENCE DEFICIENT IN ABSICSSION, a proteolytically processed peptide ligand, activating the expression of genes encoding secreted cell wall remodeling and hydrolase enzymes. *hae hsl2* mutants fail to induce expression of these genes and retain floral organs indefinitely. Here, we report identification of an allelic series of *hae hsl2* suppressor mutations in the *SERK1* coreceptor protein kinase gene. Genetic and transcriptomic evidence indicates that these alleles represent a novel class of gain-of-function mutations that activate signaling independently of HAE/HSL2. We show that, surprisingly, the suppression effect does not rely on the protein kinase activity of SERK1 and that activation of signaling relies on the receptor-like kinase gene *SUPPRESSOR OF BIR1* (*SOBIR1*). The effect of these mutations can be mimicked by loss of function of *BAK1-INTERACTING RECEPTOR-LIKE KINASE1* (*BIR1*), a known negative regulator of *SERK-SOBIR1* signaling. These results suggest that *BIR1* negatively regulates *SERK-SOBIR1* signaling during abscission and that the identified *SERK1* mutations likely interfere with this negative regulation.

Abscission is the process by which plants shed structures, such as fruit, leaves, and floral organs. Abscission occurs as the result of a developmental process or is triggered by damage or adverse environmental conditions. In Arabidopsis (*Arabidopsis thaliana*), abscission of sepals, petals, and stamen follows pollination in a developmentally programmed manner, while abscission of cauline leaves occurs as a result of drought stress or pathogen infection (Patterson, 2001; Liljegren et al., 2009; Patharkar and Walker, 2016; Patharkar et al., 2017). Abscission is regulated by the two redundant Leu-rich repeat receptor-like protein kinases (RLKs), HAESA and HAESA-LIKE2 (HAE/HSL2; Jinn et al., 2000; Cho et al., 2008; Stenvik et al., 2008). Binding of the proteolytically processed, secreted peptide INFLORESCENCE-DEFICIENT IN ABSCISSION (IDA) induces the association of HAE/HSL2 and members of the SOMATIC EMBRYOGENESIS RECEPTOR-LIKE KINASE (SERK) family of Leu-rich repeat RLK coreceptors (Meng et al., 2016; Santiago et al., 2016; Schardon et al., 2016). This association activates a downstream MAP kinase cascade composed of MAP kinase kinase 4 and 5 (MKK4/MKK5) and MAP kinase 3 and 6 (MPK3/MPK6; Cho et al., 2008; Meng et al., 2016). This MAP kinase cascade targets transcriptional repressors of the AGAMOUS-like family, including AGL15, leading to derepression of *HAE* expression and an increase in signaling via positive feedback (Fernandez et al., 2000; Adamczyk et al., 2007; Chen et al., 2011; Patharkar and Walker, 2015). This signaling pathway regulates expression of several genes involved in cell wall remodeling and hydrolysis of cell wall and middle lamella polymers such as pectin (Niederhuth et al., 2013b). Plants with mutations in *HAE/HSL2* or *IDA*, or in high-order mutants of *SERK* genes, display floral abscission defects indicative of a failure to properly break down the middle lamella between the abscising organ and the body of the plant (Butenko et al., 2003; Cho et al., 2008; Meng et al., 2016). Additionally,

[1]Author for contact: walkerj@missouri.edu.
[2]Senior author.
The author responsible for distribution of materials integral to the findings presented in this article in accordance with the policy described in the Instructions for Authors (www.plantphysiol.org) is: John C. Walker (walkerj@missouri.edu).

I.T. designed, performed, and analyzed the results of experiments and wrote the article; J.B. performed the in vitro autophosphorylation assays; R.C. performed genetic analyses; J.C.W. oversaw the work and edited the article; all authors edited and approved the final version of the article.
www.plantphysiol.org/cgi/doi/10.1104/pp.18.01328

mutants in the ADP-Ribosylation Factor GTPase Activating Protein gene *NEVERSHED* (*NEV*) are also abscission deficient and possess a disorganized secretory system in the abscission zone (Liljegren et al., 2009). The abscission-deficient phenotype of *nev* can be suppressed by mutations in *SERK1* as well as mutations in the RLK gene *SUPPRESSOR OF BIR1-1* (*SOBIR1*; also known as *EVERSHED* [*EVR*]) and the cytosolic RLK *CAST AWAY* (Leslie et al., 2010; Burr et al., 2011). The exact cause of the *nev* mutant phenotype, as well as the mechanism of *nev* suppression, are not fully understood. Recent work has demonstrated that *nev* mutants have ectopic lignification patterns in the abscission zone and exhibit widespread transcriptional reprogramming, including strong induction of biotic stress response gene expression (Lee et al., 2018; Taylor and Walker, 2018). These results together suggest that the *nev* phenotype may be related to misregulation of molecular signaling, possibly involving a pathway regulating lignification of the abscission zone.

In this work, we sought to understand additional regulators of abscission signaling using a genetic suppression approach. We identified an allelic series of putative gain-of-function *SERK1* mutations capable of suppressing the abscission defect of *hae hsl2*. These mutant alleles represent a novel class of hypermorphic *SERK* gene mutations that appear to signal through the RLK *SOBIR1*, likely by interfering with the function of the negative regulator of signaling *BAK1-INTERACTING RECEPTOR-LIKE KINASE1* (*BIR1*). These alleles provide insights into the regulation of downstream signaling processes by SERK proteins. Implications for understanding of the *nev* mutant are discussed.

RESULTS

Identification of *hae-3 hsl2-3* Suppressor Mutations in the *SERK1* Gene

To identify regulators of abscission signaling, we performed suppressor screens of the previously described *hae-3 hsl2-3* abscission-deficient mutant (Niederhuth et al., 2013a, 2013b). We isolated three strong suppressors, an intermediate suppressor, and a weak suppressor. Initial mapping by sequencing of a strong suppressor identified a semidominant, linked missense mutation in the *SERK1* gene, substituting Leu-326 for Phe (Fig. 1; Supplemental Table S1). Additional genetic analysis demonstrated that all five mutants contained semidominant, linked missense mutations affecting conserved SERK protein residues (Fig. 1; Supplemental Fig. S1; Supplemental Table S1).

To gain insight into the possible functions of the mutated residues, we mapped them onto a model of the SERK1 intracellular domain based on the crystal structure of the closely related BAK1/SERK3 protein kinase domain as well as on the recently solved crystal structure of the SERK1 ectodomain (Yan et al., 2012; Santiago et al., 2013; Protein Data Bank IDs 3ULZ and 4LSC). The four protein kinase domain mutations are localized to a patch of three surface-exposed residues on the N-lobe of the protein kinase domain distal to the catalytic cleft (Fig. 1). The phenotypes of these mutants are all strong or intermediate (Supplemental Fig. S1; Supplemental Table S1). The extracellular domain mutation with the weak suppression phenotype maps to the ligand receptor-binding face of the ectodomain (Fig. 1). This residue, Arg-147, makes side chain interactions with the residue Asp-123, which is homologous to BAK1 residue Asp-122. Mutation of Asp-122 yields a hypermorphic variant of BAK1 displaying ligand-independent association with the brassinosteroid receptor BRI1 and reduced affinity for the ectodomain of members of the BIR family of negative regulators of signaling (Jaillais et al., 2011; Hohmann et al., 2018). However, we found the weak phenotype of this mutant difficult to study and instead focused on the intracellular domain mutants. Since the four strongest mutations cluster to a spatially restricted region of the protein kinase domain, we hypothesize that the mutations have a similar effect. To study this effect, we examined the *serk1-L326F* mutant as a representative allele.

Genetic Analysis of *hae-3 hsl2-3 serk1-L326F*

Because *SERK1* positively regulates abscission and because these mutations are all semidominant, we hypothesized that they are gain-of-function mutations. We performed several genetic experiments to test this hypothesis. We first crossed the *hae-3 hsl2-3* mutant

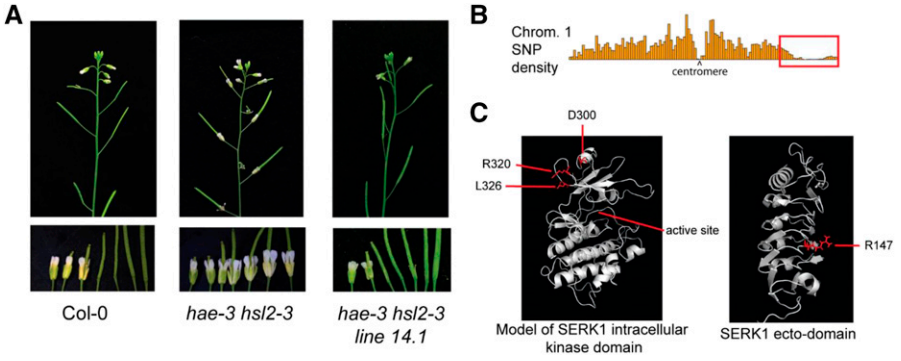

Figure 1. Phenotypes and molecular mapping of *hae-3 hsl2-3* suppressor mutations. A, Floral abscission phenotypes of Columbia-0 (Col-0), *hae-3 hsl2-3*, and *hae-3 hsl2-3 line 14.1*. B, Landsberg *erecta* (Ler) single-nucleotide polymorphism (SNP) density resulting from mapping by sequencing of bulked DNA from strongly abscising *hae hsl2 line 14.1* (Col-0) × *hae hsl2* (Ler) F2 plants, indicating linkage to chromosome 1. C, Predicted location of *hae hsl2* suppressor mutations on the SERK1 protein.

with the well-characterized *serk1-1* loss-of-function transfer DNA (T-DNA) insertion mutant. Consistent with previously published analysis of *serk1* loss-of-function mutations (Lewis et al., 2010), we found that the *serk1-1* allele is unable to suppress the abscission defect of *hae-3 hsl2-3*, demonstrating specificity of the suppression defect to the semidominant alleles isolated in our screen (Fig. 2). We next crossed the *serk1-L326F* mutant with the *hae-1 hsl2-4* double mutant. This mutant has a T-DNA insertion in the first exon of *HAE* and a premature stop codon in the first exon of *HSL2* and is a predicted protein null (Niederhuth et al., 2013a). We isolated the *hae-1 hsl2-4 serk1-L326F* triple mutant and found that it displays nearly complete suppression of the abscission defect similar to *hae-3 hsl2-3 serk1-L326F*, demonstrating nonspecificity of the suppression effect with regard to alleles of *hae* and *hsl2* (Fig. 2). We further performed a transgenic recapitulation experiment, where we transformed *SERK1pr*::*SERK1* wild-type and *SERK1pr*::*SERK1-L326F* mutant transgenes into *hae-3 hsl2-3*. In the T1 generation, we found that none of 16 plants transformed with the wild-type transgene displayed abscission (Fig. 2; Supplemental Table S2 for all transgene counts). For the *SERK1pr*::*SERK1-L326F* transgene, 10 of 30 T1 plants displayed weak or strong suppression (Fig. 2; Supplemental Table S2). These results are consistent with a model wherein *serk1-L326F* is a hypermorphic mutation.

Next, we tested whether the *serk1-L326F* mutation interferes with the normal functions of *SERK1*. Prior work has shown that the *serk1-1 serk2-1* double loss-of-function mutant is male sterile because of defective tapetum development and that the *serk1-1 serk2-1 bak1-5* triple mutant is sterile and displays a weak abscission defect (Albrecht et al., 2005; Colcombet et al., 2005; Meng et al., 2016). We regenerated the *serk1-1 serk2-1 bak1-5* triple mutant and confirmed the sterility and abscission-defective phenotypes (Fig. 2). We also created the *serk1-L326F serk2-1 bak1-5* triple mutant and found that it displays wild-type fertility and abscises all its floral organs, indicating that the *serk1-L326F* mutant allele is a functional coreceptor in tapetum development and abscission (Fig. 2).

Next, we examined the effect of the *serk1* suppressor mutations in relation to downstream signaling processes. Previously published MAP kinase signaling suppression strategies used in floral abscission research involve inefficient tandem RNA interference targeting *MKK4/MKK5* or complicated *MPK3/MPK6* transgenic/mutant combinations (Cho et al., 2008). Work in stomatal cellular identity specification has shown that MAP kinase signaling regulated by MKK4/MKK5-MPK3/MPK6 can be suppressed in a cell type-specific manner by expression of a kinase-inactive version of the MAPKKK *YODA* (*YDA*) gene (Lampard et al., 2009). The identity of the MAPKKK(s) upstream of MKK4/MKK5 during floral abscission is unknown. Nonetheless, we hypothesized that expression of kinase-inactive *YDA* under the control of the *HAE* promoter may block signaling by MKK4/MKK5 during floral abscission.

To test this approach, we created a *HAEpr*::*YDA-YFP K429R* construct designed to express a YDA-YFP fusion with a mutation of a conserved, catalytic Lys specifically in the abscission zone. We found that 33 of 64 T1

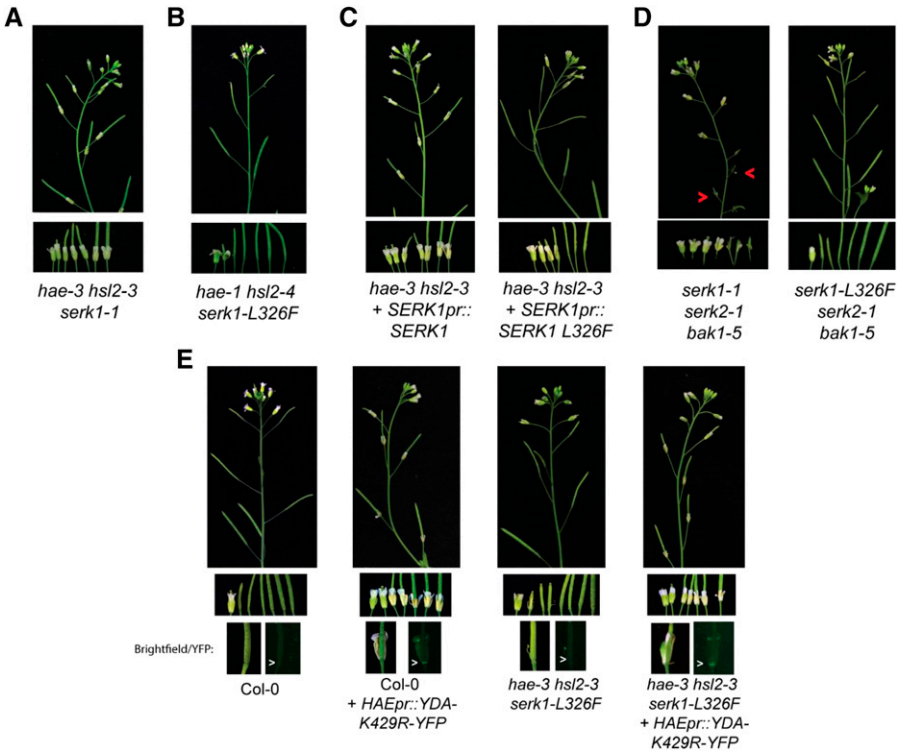

Figure 2. Genetic analysis of a representative hypermorphic *SERK1* allele. A, Phenotype of the *hae-3 hsl2-3 serk1-1* triple mutant. B, Phenotype of the *hae-1 hsl2-4 serk1-L326F* triple mutant. C, Transgenic recapitulation of the *hae hsl2* suppression phenotype (T1 generation). D, Phenotypes of *serk1 serk2 bak1* triple mutants. E, Phenotypes of *HAEpr::YDA-YFP K429R* transformed into Col-0 and *hae-3 hsl2-3 serk1-L326F* (T1 generation).

plants transformed with this construct in the Col-0 background displayed abscission defects similar to *hae hsl2* mutants (Fig. 2; Supplemental Table S2). This phenotype is associated with YFP signal restricted to the abscission zone, where HAE is normally expressed (Fig. 2). We next tested the ability of this construct to block the suppression effect of *hae-3 hsl2-3 serk1-L326F*. We found that eight of 14 T1 *hae-3 hsl2-3 serk1-L326F HAEpr::YDA-YFP K429R* plants had abscission defects similar to *hae hsl2* mutants (Fig. 2; Supplemental Table S2). These results indicate that the suppression effect acts upstream of MAP kinase signaling, which is consistent with our hypothesis of hypermorphic activation of signaling at the plasma membrane. These results also provide circumstantial evidence that YDA acts downstream of the HAE/HSL2-SERK complex.

RNA Sequencing of Col-0, *hae-3 hsl2-3*, and *hae-3 hsl2-3 serk1-L326F*

We next performed an RNA sequencing (RNA-Seq) experiment on floral receptacle-derived RNA to examine the transcriptome of the *hae-3 hsl2-3 serk1-L326F* mutant in relation to the parental *hae-3 hsl2-3* mutant and the grandparental Col-0. We hypothesized that the *serk1* suppressor would exhibit a reversion of gene expression levels from the *hae-3 hsl2-3* parent toward the Col-0 grandparent (output of differential expression analysis in Supplemental Data Set S1).

First, we assessed transcript abundance measurements for the *HAE/HSL2* marker genes *QRT2* and *PGAZAT* (Fig. 3). These genes encode polygalacturonases involved in the breakdown of pectin in the middle lamella (Ogawa et al., 2009). The double *qrt2 pgazat* mutant exhibits a weak abscission delay, and expression of these genes is strongly reduced in the *hae hsl2* mutant (Ogawa et al., 2009; Niederhuth et al., 2013b). Thus, we consider the expression of these genes useful markers for *HAE/HSL2* pathway activity, although it should be noted that they are likely only two of many functionally relevant hydrolase genes regulated by *HAE/HSL2*. Consistent with the hypothesis that the *hae-3 hsl2-3 serk1-L326F* mutant is gain of function, the transcript abundance of *QRT2* is increased to an approximately wild-type level (Fig. 3). In contrast, *PGAZAT* has a greater than 5-fold increase compared with the wild-type grandparent (Fig. 3). These results are consistent with a model where there is activation of a *SERK1*-regulated abscission signaling pathway in the *hae-3 hsl2-3 serk1-L326F* mutant.

To detect global patterns in gene expression changes in the *hae-3 hsl2-3 serk1-L326F* mutant, we performed Gene Ontology (GO) analysis comparing all three genotypes (Supplemental Table S3). The most statistically significant findings are terms enriched in the Col-low/*hae-3 hsl2-3 serk1-L326F*-high and *hae-3 hsl2-3*-low/*hae-3 hsl2-3 serk1-L326F*-high comparisons and include genes associated with terms such as response to stimulus, response to stress, and response to biotic stimulus, among other terms associated with response to biotic stress (partial list in Table 1). Overall, these results suggest that there is a *SERK1*-mediated signaling pathway overactivated in *hae-3 hsl2-3 serk1-L326F* regulating both abscission and biotic stress response signaling.

As an additional control, we performed an RNA-Seq experiment comparing Col-0 with the single loss-of-function mutant *serk1-1* and the single putative gain-of-function mutant *serk1-L326F*. In this experiment, we observed a moderate but statistically significant reduction in expression for *QRT2* and *PGAZAT* in the loss-of-function *serk1-1* mutant compared with the wild type (Fig. 3). The magnitude of this effect was less than that observed in the *hae hsl2* double mutant, consistent with a model where *SERK1* is one of a set of redundant *SERK* genes regulating abscission. In contrast, in the *serk1-L326F* single mutant, we observed a statistically

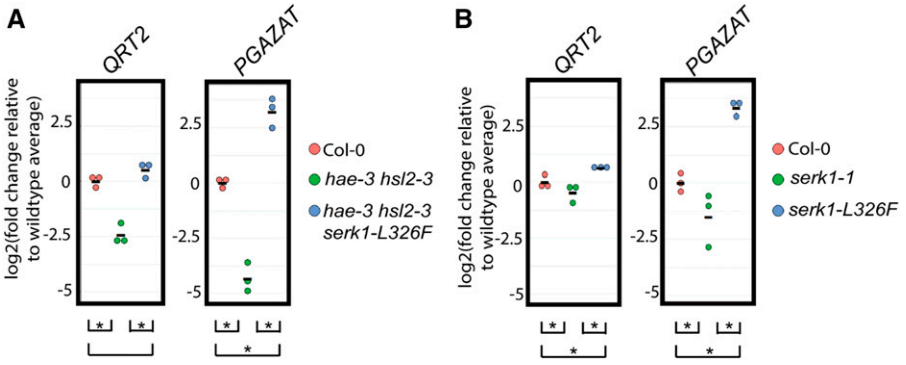

Figure 3. Transcript abundance measurements for abscission hydrolase genes *PGAZAT* and *QRT2*. A, Log2(fold change) relative to wild-type average fragments per kilobase per million reads for abscission hydrolase genes *QRT2* and *PGAZAT*. $n = 3$ observations from tissue isolated from three independent pools of plants. Asterisks denote $P < 0.05$ at false discovery rate (FDR) of 0.05. B, Log2(fold change) relative to wild-type average fragments per kilobase per million reads for abscission hydrolase genes *QRT2* and *PGAZAT*. $n = 3$ observations from tissue isolated from three independent pools of plants. Asterisks denote $P < 0.05$ at FDR of 0.05.

Table 1. *GO terms associated with differentially expressed genes in Col-low/*hae-3 hsl2-3 serk1-L326F-*high and Col-low/*serk1-L326F-*high comparisons*

Description	FDR
Col-low/*hae-3 hsl2-3 serk1-L326F*-high	
Response to stimulus	1.2E-93
Response to stress	1.8E-80
Response to biotic stimulus	3.3E-65
Multiorganism process	1.6E-57
Response to external stimulus	2.3E-56
Response to endogenous stimulus	6.3E-29
Cell communication	1.1E-28
Signal transduction	2.5E-27
Cell death	2E-17
Secondary metabolic process	3.9E-14
Col-low/*serk1-L326F*-high	
Response to stimulus	1E-51
Response to stress	4.4E-37
Response to biotic stimulus	1.6E-36
Response to external stimulus	7.8E-33
Multiorganism process	2.3E-32
Response to endogenous stimulus	2.3E-14
Response to abiotic stimulus	2.3E-14
Secondary metabolic process	6E-11
Cell communication	4.4E-08
Catabolic process	5.4E-08

significant increase in both *QRT2* and *PGAZAT* expression compared with the wild type (Fig. 3). These results are consistent with a model where *SERK1* positively regulates abscission signaling and the *serk1-1* and *serk1-L326F* mutations are loss of function and gain of function, respectively.

In addition, in the Col-low/*serk1-L326F*-high and *serk1-1*-low/*serk1-L326F*-high comparisons, GO analysis identified a strong enrichment in terms such as response to stimulus, response to stress, and response to biotic stimulus, similar to the *hae-3 hsl2-3 serk1-L326F* mutant (Table 1; Supplemental Table S3). These results are consistent with a model *serk1-L326F* mutant as a gain-of-function allele broadly activating intracellular signaling. Additionally, we performed quantitative phenotyping of the wild type compared with the single *serk1-1* and *serk1-L326F* mutants (Supplemental Fig. S2). We observed that wild-type abscission occurred at a median floral position between 4 and 5 (floral position 1 is defined as the first flower postanthesis, with each older flower increasing in position by 1; Supplemental Fig. S2). We observed the *serk1-L326F* mutant abscising slightly earlier than the wild type at median floral position 4, although this difference was not statistically significant (Supplemental Fig. S2). The single *serk1-1* mutant, in contrast, abscised at a median position of 6, which is highly statistically significantly delayed compared with both the wild type and *serk1-L326F* (Supplemental Fig. S2). These results further support that there is a reduction in signaling in the loss-of-function *serk1-1* mutant. They also suggest that, in *serk1-L326F*, enhanced signaling does not appear to dramatically alter the timing of abscission compared with the wild type. Interestingly, for both the *serk1-L236F* single mutant and the *hae-3 hsl2-3 serk1-L326F* suppressor mutant, we observed enlarged and disordered abscission zones following abscission by floral position 10, suggesting that signaling is not being properly regulated and/or attenuated (Supplemental Fig. S2).

The sum of these results indicates that these *SERK1* suppressor mutations are hypermorphic and induce signaling downstream of the plasma membrane through a MAP kinase cascade. This signaling activates broad transcriptional reprogramming, including genes associated with cell wall modification during abscission, as well as biotic stress response signaling.

The Suppression Effect Does Not Require SERK1 Protein Kinase Activity

We next investigated potential biochemical mechanisms of *hae hsl2* suppression by the *SERK1* mutations. We hypothesized that the protein kinase domain mutations might overactivate the SERK1 protein kinase domain, causing constitutive phosphorylation of cellular substrates. Contrary to this hypothesis, in vitro autophosphorylation analysis did not identify a difference in the autophosphorylation level between wild-type SERK1 and the three protein kinase domain mutations with the strongest suppression effect (Fig. 4). This result suggests that these mutations do not alter intrinsic protein kinase activity of the SERK1 protein.

We next hypothesized that the *serk1* suppressor mutations alter a negative regulatory interaction in vivo that allows SERK1 to phosphorylate cellular substrates constitutively in a manner that does not alter SERK1 protein kinase activity. To test this hypothesis genetically, we used site-directed mutagenesis to create a *SERK1pr*::*SERK1-L326F K330R* transgene. This double mutant lacks an invariant catalytic Lys found in all protein kinases and lacks autophosphorylation activity in vitro (Supplemental Fig. S3). We hypothesized that this mutant would be unable to suppress the abscission-defective *hae hsl2* phenotype due to abolition of its protein kinase activity. However, in the T1 generation, we found a spectrum of *hae-3 hsl2-3* suppression phenotypes similar to the *SERK1pr*::*SERK1-L326F* single mutant T1 generation plants (~45% strong or partial suppression in 22 lines; Fig. 4; Supplemental Table S2). We discovered that this effect also occurs with a version of *SERK1-L326F K330R* tagged with 2xHA (Supplemental Fig. S3). These results indicate that phosphorylation of a cellular substrate by the mutant kinase is not the cause of the suppression effect. We speculate that these mutations activate a SERK-guarding or -monitoring mechanism that senses some biochemical alteration of SERK proteins to transduce a signal downstream, independent of protein kinase activity.

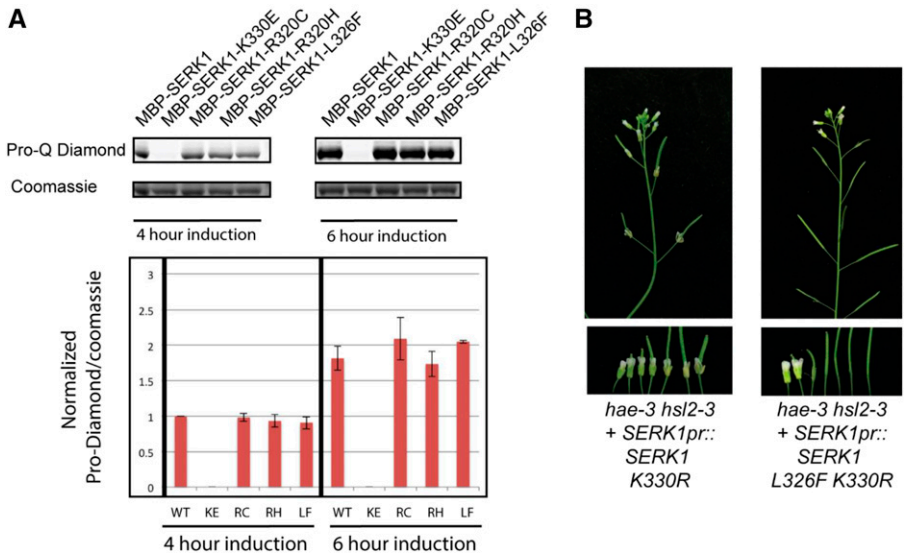

Figure 4. Analysis of kinase activity on the *hae-3 hsl2-3* suppression effect. A, In vitro autophosphorylation after 4 and 6 h of induction of recombinant MALTOSE BINDING PROTEIN (MBP)-SERK1 intracellular domain fusion proteins. $n = 3$ replicate cultures. Error bars represent SE. WT, Wild type. B, Phenotypes of transgenic *hae-3 hsl2-3* transformed with single and double mutant kinase-inactive, untagged variants of *SERK1* (T1 generation).

Evidence That *SOBIR1* Transduces Signaling Downstream of *SERK1* in *hae-3 hsl2-3 serk1-L326F*

We next sought to understand downstream signaling mechanisms in the suppressor mutant. Recent work has shown that overexpression of a *BAK1* transgene lacking the cytosolic kinase domain can activate pathogen response signaling via the RLK *SOBIR1* (Domínguez-Ferreras et al., 2015). This result is reminiscent of our observation that signaling by *serk1-L326F* can induce intracellular signaling independent of the protein kinase activity of SERK1. In addition, *SOBIR1* is specifically expressed in abscission zones and has been previously implicated in the regulation of floral abscission (Leslie et al., 2010). Thus, we hypothesized that *SOBIR1* may function downstream of the suppressor mutations.

To test this model, we crossed the *hae-3 hsl2-3 serk1-L326F* mutant with the exonic *SOBIR1* T-DNA mutant *sobir1-12/evr-3*. This mutant allele has previously been reported to suppress the abscission defect of *nev-3* (Gao et al., 2009; Leslie et al., 2010). We hypothesized that SOBIR1 transduces signaling downstream of SERK1, and thus a *sobir1* mutation would block the effect of the *serk1-L326F* mutation. In the F3 generation, we identified two quadruple homozygous individuals for the four mutations exhibiting strong abscission deficiency (Fig. 5). These results suggest that *SOBIR1* transduces the signal downstream of the *serk1-L326F* mutation.

We performed quantitative PCR (qPCR) on the *hae-3 hsl2-3 serk1-L326F sobir1-12* quadruple mutant and compared it with the *hae-3 hsl2-3 serk1-L326F* parent. We utilized a paired design where the difference of the normalized threshold counts for the two genotypes is calculated for each replicate to create a univariate relative gene expression measure. The null hypothesis is that there are no differences between the genotypes and the subtracted threshold counts will be centered around zero. The alternative hypothesis is that the differences will be centered around a nonzero value. We found that the abscission-associated hydrolase *PGAZAT* had, on average, an approximately log2(fold change) difference of 3, corresponding to an approximately 8-fold decrease of transcript abundance in the quadruple *hae-3 hsl2-3 serk1-L326F sobir1* mutant (Fig. 5). We also tested the pathogen response marker *PR2* and found that it exhibited an average log2(fold change) difference of 4, corresponding to an approximately 16-fold decrease in transcript abundance of *PR2* in the quadruple mutant. Overall, these results confirm that there is a reduction in both abscission and pathogen signaling in the quadruple mutant (Fig. 5).

To confirm that the quadruple mutant phenotype is caused by the mutation in *SOBIR1*, we transformed the quadruple mutant with a transgene expressing either the wild-type *SOBIR1* coding sequence fused to a FLAG tag or the same transgene with a mutation in the conserved catalytic Lys-377. We observed that the wild-type transgene complemented the abscission-deficient phenotype in a majority of T1 lines (58% of 36; Supplemental Table S2), whereas the K377R mutant did not complement any T1 lines examined (zero of 25; Fig. 5; Supplemental Table S2). We screened and found similarly expressing wild-type and K377R lines assayed with an anti-FLAG antibody (Fig. 5). Thus, *SOBIR1* can transduce the abscission signal downstream of *serk1-L326F* in a protein kinase activity-dependent manner.

Evidence That BIR1 Negatively Regulates Abscission Signaling

Next, we sought to understand the mechanism by which the identified *serk1* suppressor mutations might function through *SOBIR1*. The protein kinase BIR1 has been identified as an interactor of SERK proteins (Gao et al., 2009). In *bir1* mutants, pathogen response signaling is constitutively activated, leading to extreme

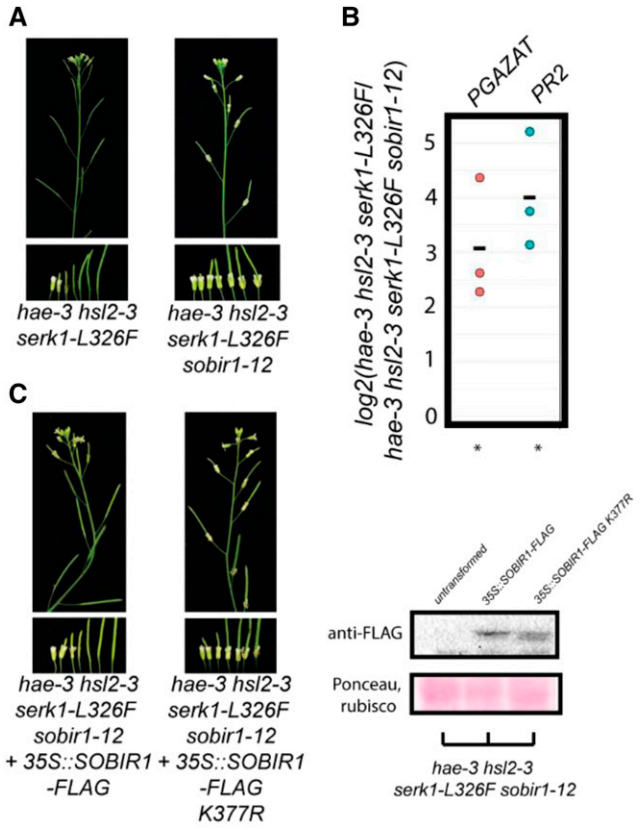

Figure 5. Evidence that *SOBIR1* functions downstream of *SERK1* during abscission signaling. A, Phenotypes of *hae-3 hsl2-3 serk1-L326F* and *hae-3 hsl2-3 serk1-L326F sobir1-12*. B, Estimated log2(fold change) of transcript abundance measurements between *hae-3 hsl2-3 serk1-L326F* and *hae-3 hsl2-3 serk1-L326F sobir1-12* for abscission hydrolase *PGAZAT* and pathogen response marker *PR2*. Asterisks denote $P < 0.05$. C, Transgenic complementation of the *hae-3 hsl2-3 serk1-L326F sobir1-12* phenotype relies on kinase activity of SOBIR1 (T1 generation).

dwarfism and seedling lethality (Gao et al., 2009). This effect can be partially suppressed by mutation in *SOBIR1* (Gao et al., 2009). Thus, BIR1 is thought to negatively regulate signaling by SOBIR1, possibly by acting in a guard complex. Based on these previously known genetic interactions, we hypothesized that BIR1 may negatively regulate signaling during abscission and that loss of function of *BIR1* may lead to activation of SOBIR1 in abscission zones in a similar manner to that of *serk1-L326F*.

To test this hypothesis, we sought to combine the *hae hsl2* double mutant with a loss-of-function *bir1* mutant. We hypothesized that these plants would overactivate the SERK1-SOBIR1 abscission pathway and would therefore exhibit restored abscission and enhanced biotic stress response gene expression. *bir1* null mutants are extremely dwarfed and typically die before flowering under standard growth conditions, rendering floral genetic studies difficult. As an alternative, artificial microRNA (amiRNA) targeting *BIR1* has been shown to effectively mimic loss-of-function mutations in *BIR1* (Gao et al., 2009). Therefore, we created two related *BIR1* amiRNA constructs driven either by the *HAE* promoter alone or by a tandem *35S*::*HAEpr*. We anticipated that the *HAEpr* would provide adequate expression levels in the abscission zone, while the tandem *35S*::*HAEpr* would boost expression in abscission zones in the event that the *HAEpr* proved too weak to be effective.

In the T1, we found that two of 26 *35S*::*HAEpr*::*amiRNA-BIR1* plants exhibited partial suppression of the *hae-3 hsl2-3* abscission phenotype, as well as semidwarfism with yellowed leaves, while for *HAEpr*::*amiRNA-BIR1*, one of 16 plants exhibited similar partial abscission, yellow leaves, and semidwarfism (Fig. 6; Supplemental Table S2). Thus, loss of *bir1* function appears to suppress the *hae hsl2* abscission defect, phenocopying the gain-of-function mutation *serk1-L326F*. The leaf phenotype and semidwarfism are consistent with weak activation of autoimmunity. To examine these lines, we grew the T2 of one of the *35S*::*HAEpr* lines and performed qPCR on RNA derived from the floral receptacle on *BIR1* to examine the accumulation of transcript. Across three biological replicates, we observed a statistically significant log2(fold change) of 0.66 for *BIR1* between *hae-3 hsl2-3* and *hae-3 hsl2-3 amiRNA-BIR1*, corresponding to an approximately 40% reduction in *BIR1* transcript accumulation (Fig. 6). We also tested transcript abundance of *PGAZAT* and *PR2* and found an approximate log2(fold change) of five and 5.4 between *hae-3 hsl2-3* and *hae-3 hsl2-3*

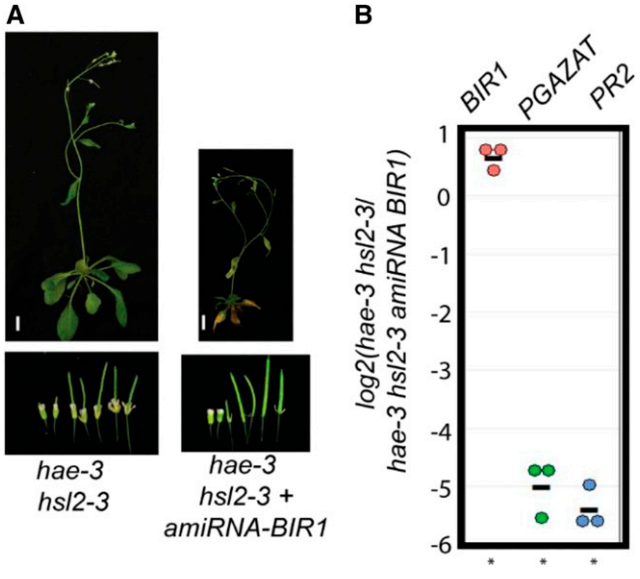

Figure 6. Evidence that *BIR1* negatively regulates abscission signaling. A, Phenotypes of *hae-3 hsl2-3* and partially suppressed *hae-3 hsl2-3 + HAEpr*::*amiRNA BIR1* (T1 generation). Bars = 1 cm. B, Estimated log2(fold change) of transcript abundance measurements between *hae-3 hsl2-3* and *hae-3 hsl2-3 amiBIR1* for *BIR1*, abscission hydrolase *PGAZAT*, and pathogen response marker *PR2*. Asterisks denote $P < 0.05$.

amiBIR1 for both genes, respectively, which corresponds to approximately 32- and 42-fold increases in expression of both genes in the *amiRNA-BIR1* line (Fig. 6). These results are consistent with a model where *BIR1* negatively regulates abscission signaling and that loss of function of *BIR1* leads to high levels of abscission and biotic stress response gene expression, in a manner similar to the *serk1-L326F* mutations.

DISCUSSION

In this work, we have shown that a particular class of hypermorphic *SERK1* mutations broadly activate intracellular signaling via the RLK *SOBIR1*. The phenotype of these *hae hsl2* suppressor mutations in *SERK1* can be phenocopied by loss of function of the negative regulator of signaling *BIR1*. Prior work has provided strong evidence that the function of BIR1 is to bind to SERK proteins and inhibit the activation of multiple pathways, including one regulated by *SOBIR1*. Taken together, these data suggest that BIR1 functions in abscission to inhibit overactivation of signaling by SOBIR1. These mutations should provide powerful insight into the activation of SOBIR1 and the regulation of this process by BIR1.

Prior work has shown that *SOBIR1* is specifically expressed in floral abscission zones and that it is globally coexpressed with *HAE* (Leslie et al., 2010; Patharkar and Walker, 2015). This, combined with the genetic data presented in this study, suggests that *SOBIR1* contributes to wild-type abscission signaling downstream of the SERK proteins. We hypothesize that the function of BIR1 during abscission is to moderate SERK-mediated activation of SOBIR1 to prevent overactivation of signaling. We further hypothesize that the *serk1* suppressor mutations isolated in this screen interfere with the function of BIR1 by an unknown mechanism. Testing these hypotheses is a clear direction for future research. Notably, the single *sobir1* mutant does not have an abscission defect (Leslie et al., 2010). This implies that there are parallel pathways regulating abscission downstream of the HAE/HSL2-SERK complex. An alternative explanation for these results is that, rather than act as a bona fide regulator of abscission signaling, SOBIR1 activation may instead be an undesired by-product of the activation of the SERK protein signaling complex, and this spurious activation of SOBIR1 may be promoted by the *serk1* suppressor mutations identified in this screen. In this case, the function of BIR1 may simply be to prevent SERK protein-mediated activation of SOBIR1 altogether as a way to counteract this inadvertent signal. Given the specific expression pattern of *SOBIR1* in floral abscission zones, this possibility seems unlikely, but it is one that cannot be ruled out until additional genetic evidence defining hypothetical parallel pathways including *SOBIR1* comes to light.

This work also provides possible insight into the phenotype of the *nev* mutant. We have recently shown that the *nev* mutant exhibits widespread transcriptional reprogramming, including extensive induction of biotic stress response gene expression, and that this transcriptional reprogramming is partially reversed in the *nev serk* suppressor line (Taylor and Walker, 2018). Thus, it appears that there may be an aberrant signaling process regulated by *SERK1* that is activated in *nev* that interferes with abscission zone function. This aberrant transcriptional reprogramming is reminiscent of that observed in the *serk1-L326F* mutant. Because loss-of-function mutations in both *SERK1* and *SOBIR1* can suppress the abscission defect of *nev*, this is evidence that the same pathway activated in the *hae hsl2 serk1* suppressor mutants described in this article is activated in *nev*. Recent work has shown that the *nev* mutant exhibits overlignification of the abscission zone (Lee et al., 2018). This overlignification may be the result of aberrant signaling in *nev* and could plausibly interfere with normal cell wall modifications required for abscission. Thus, overlignification represents one possible physical explanation for the phenotype of the *nev* mutant. Why the activation of signaling would yield differing phenotypes in *nev* and the *hae hsl2 serk1* suppressor mutants identified in this screen is an important question that will require additional research. It may be that cellular defects of the *nev* mutant render it more susceptible to abscission zone malfunction, or that aberrant signal intensity is higher in *nev*, or a combination of both. Much more work remains to understand *nev* and its suppressors as well as their relationship to the *serk1* mutants identified in this screen, but this work will help guide future investigations in this area.

MATERIALS AND METHODS

Lines Used in This Study

Arabidopsis (*Arabidopsis thaliana*) mutants *serk1-1* (SALK_044330C), *serk2-1* (SALK_058020C), and *sobir1-12* (SALK_ 050715) were obtained from the Arabidopsis Biological Resource Center (Alonso et al., 2003; Albrecht et al., 2005; Colcombet et al., 2005; Gao et al., 2009; Leslie et al., 2010). *hae-3 hsl2-3*, *hae-3 hsl2-3 serk1-L326F*, and *hae-3 hsl2-3 serk1-L326F sobir1-12* have been deposited in the Arabidopsis Biological Resource Center. The *hae-3 hsl2-3 serk1-L326F* mutant was backcrossed to Col-0 five times. High-order mutant combinations were created by cross. All primers used in this study are listed in Supplemental Table S4.

Plant Growth Conditions

All plants with the exception of the Col-0/*serk1-1/serk1-L326F* RNA-Seq and abscission quantification experiment were grown in a 16-h light cycle, ~125 μE m^{-2} s^{-1}, at 22°C. Col-0/*serk1-1/serk1-L326F* RNA-Seq plants were grown in a 16-h light cycle, ~60 μE m^{-2} s^{-1}, 23°C. Col-0/*serk1-1/serk1-L326F* abscission quantification plants were grown in a 16-h light cycle, ~150 μE m^{-2} s^{-1}, 22°C. All plants were fertilized once at 3 weeks postgermination with 1× strength Miracle-Gro (Scotts Miracle-Gro).

Phenotyping

Qualitative suppression phenotypes were determined by lightly brushing the main inflorescence of young (less than 2 weeks post bolting) plants to remove remnant, abscised floral organs and classifying them according to highest similarity to *hae-3 hsl2-3* (nonsuppressed), *hae-3 hsl2-3 serk1-L326F*/+ (partial

suppression), and *hae-3 hsl2-3 serk1-L326F* (strong suppression). Phenotyping of transgenic lines was performed in the T1 generation.

Quantitative phenotyping of Col-0, *serk1-1*, and *serk1-L326F* was performed by utilizing our previously described petal-puller assay (Baer et al., 2016). In this assay, two paintbrushes are affixed at an angle to a rigid rod, with spacers present to create a consistent amount of force applied. We lightly dragged the inflorescence of plants at ~2 weeks post bolting, then rotated the plants 90°, and performed the procedure again. The objective of this assay is to remove all remnant floral organs that have undergone abscission but are still loosely attached. Next, we counted the number of flowers that had nonabscised floral organs, starting from position 1. The first silique in which all floral organs had abscised was recorded. We performed this analysis for 10 plants of each genotype grown in the same flat. We performed a Wilcoxon rank-sum test on the floral positions to test for a shift in location of the median position of abscission.

RNA-Seq

RNA from six to 15 pooled stage 15 preabscission receptacles per replicate was isolated using the Trizol reagent (Life Technologies). The number of receptacles varied based on the number of stage 15 flowers for each genotype at the time of tissue harvesting. Each receptacle was dissected by taking a 1-mm section of floral tissue composed of 0.33 mm stem and 0.67 mm receptacle. Libraries were created using the TruSeq mRNA Library Prep Kit (Illumina). Libraries from each experiment were individually barcoded and run on a single lane of Illumina Sequencing. One replicate of Col-0, *hae-3 hsl2-3*, and *hae-3 hsl2-3 serk1-L326F* was run after the second backcross of the suppressor and *hae-3 hsl2-3* mutants to Col-0 to obtain preliminary data, using the Illumina HiSeq 2500. The second and third replicates were performed on the fifth backcrosses and they, along with the Col-0/*serk1-1/serk1-L326F* experiment, were sequenced on an Illumina NextSeq 500.

Reads were mapped to TAIR 10 gene sequences and quantified using TopHat (v2.0.9) and Cufflinks (v2.1.1; Trapnell et al., 2012). We utilized default settings for alignments, and performed differential expression analyses using cuffdiff with default settings. Data were analyzed and visualized in R using ggplot2 (Trapnell et al., 2012). BAM files have been deposited at the Sequence Read Archive under BioProject accession number PRJNA430092.

The GO analyses were performed by outputting lists of genes from each comparison found to have a significant difference, with FDR set at 0.05. These lists were compared using agriGO (Du et al., 2010), using Fisher's exact test, and Yekutieli FDR under dependency, with a 0.05 significance level, against the plant GO database.

hae-3 hsl2-3 Suppressor Screen

Two suppressor mutant screens were performed on a mutant derived from a cross of *hae-3 hsl2-3* and a previously described *erecta glabra* (*er gl*) mutant, both in the Col-0 ecotype (Baer et al., 2016). *hae-3* contains a missense mutation causing the amino acid residue Cys-222 to be substituted with Tyr in the extracellular domain, leading to degradation of the mutant protein by an endoplasmic reticulum-associated protein quality-control mechanism (Niederhuth et al., 2013a; Baer et al., 2016). *hsl2-3* contains a missense mutation causing substitution of the amino acid residue Gly-360 with Arg in the HSL2 extracellular domain (Niederhuth et al., 2013a). The molecular defect of *hsl2-3* is currently unknown. We isolated the *hae-3 hsl2-3 er gl* quadruple mutant, which fails to abscise and possesses the characteristic semidwarf phenotype of an *er* mutant and lacks trichomes. We used this mutant as a background for our screens to control for any wild-type seed contamination that could interfere with suppressor identification. Its short stature makes it convenient for dense planting to screen for floral phenotypes.

We performed an ethyl methanesulfonate suppressor screen by mutagenizing 50,000 *hae-3 hsl2-3 er gl* seeds and growing 50 pools of M1 seeds. Approximately 2,000 seeds from each M1 pool were grown in the M2 to screen for mutant phenotypes. We began initial characterization of four mutants that showed moderate to strong suppression. Two strong suppressors were selected for mapping by crossing to a *hae hsl2* mutant in the L*er* ecotype. In the F2, we selected strongly suppressed individuals, pooled the DNA, and sequenced on an Illumina HiSeq. Reads were aligned with Bowtie2 (version 2.2.6), and SNPs were analyzed with SAMtools (version 0.1.19) and the Bar Toronto mutant analysis pipeline to identify a linked region in both mutants on the long arm of chromosome 1 (Li et al., 2009; Austin et al., 2011; Langmead and Salzberg, 2012). Analysis of mutations revealed that each mutant had a distinct mutation in the *SERK1* RLK gene. Since *SERK1* is implicated in regulating abscission, it was our highest candidate (Lewis et al., 2010). The other strong mutant and an intermediate mutant were shown by linkage analysis in the F2 of a cross with L*er hae hsl2* to exhibit strong linkage to the marker NGA 111 near the *SERK1* locus (Supplemental Fig. S1). Sanger sequencing of the coding regions of *SERK1* in these lines revealed additional missense mutations.

Simultaneously, we performed an activation tagging screen in which 60,000 T1 and 180,000 T2 progeny were screened for suppression of the abscission-deficient phenotype of *hae-3 hsl2-3* (Weigel et al., 2000). One line with weak suppression was shown, by thermal asymmetric interlaced-PCR and by backcross F2 segregation analysis, to have an unlinked T-DNA insertion upstream of At5g09880, a CC1-like splicing factor. However, analysis of the chromatogram of Sanger sequencing of pooled backcross F2 DNA showed a linked SNP in *SERK1* in suppressed individuals, suggesting that a spontaneous mutation arose in the *SERK1* gene during creation of this population (Supplemental Fig. S1).

Molecular Cloning

The *SERK1pr*::*SERK1* construct was created by cloning an ~5-kb fragment of the SERK1 locus including a stop codon into the pE2C entry vector using the *Not*I site. This was mutagenized by PCR to create *SERK1pr*::*SERK1-L326F* and *SERK1pr*::*SERK1-L326F K330R*. *SERK1pr*::*SERK1 2xHA* was created by mutagenizing *SERK1pr*::*SERK1* by PCR-based site-directed mutagenesis to delete the stop codon and to create an in-frame fusion of *SERK1* with 2xHA. This construct was mutagenized by PCR to create *SERK1pr*::*SERK1-2xHA L326F*, *SERK1pr*::*SERK1-2xHA K330R*, *SERK1pr*::*SERK1-2xHA L326F K330R*, and *SERK1pr*::*SERK1-2xHA L326F K330E*. All constructs were combined into the pGWB601 Gateway-compatible binary vector, transformed into *Agrobacterium tumefaciens* strain GV3101, transformed into Arabidopsis by floral dip, and selected with Basta (Clough and Bent, 1998; Nakamura et al., 2010).

Kinase inactive *HAEpr*::*YDA-YFP* was created by cloning the *HAE* promoter into pENTR-TOPO Kinase Inactive-YDA (Lampard et al., 2009). This construct was transferred to the binary vector pHGY by Gateway recombination, transformed into Arabidopsis by floral dip, and selected with hygromycin on Murashige and Skoog agar plates (Clough and Bent, 1998; Kubo et al., 2005).

MBP-SERK1 was created by PCR amplifying the intracellular domain of *SERK1* from a cDNA library created from Arabidopsis flowers using SuperScript III reverse transcriptase (Thermo Fisher). This amplicon was cloned into the *Kpn*I site of pMAL-cri and mutagenized by PCR to create pMAL-SERK1-KD-K330E, pMAL-SERK1-KD-L326F, pMAL-SERK1-KD-R330C, pMAL-SERK1-KD-R330H, and pMAL-SERK1-KD-L326F K330R.

The *35Spr*::*SOBIR1-FLAG* construct was created by PCR amplification of the *SOBIR1* gene from genomic DNA with the addition of a single C-terminal FLAG tag and stop codon. This fragment was cloned into pENTR/D-TOPO (Thermo Fisher). PCR-based mutagenesis was used to create 35Spr::*SOBIR1-FLAG K377R*. This construct was recombined into the Gateway-compatible pGWB602, which contains a 35S-driven promoter (Nakamura et al., 2010). Plants were transformed by floral dip and selected with Basta.

HAEpr::*amiRNA BIR1* and *35S*::*HAEpr*::*amiRNA BIR1* constructs were created by cloning approximately 2 kb upstream of the *HAE* gene into the *Bam*HI/*Not*I sites of the Gateway entry vector pE6c (Dubin et al., 2008). A *Pac*I site was engineered downstream of *HAEpr*. The *amiRNA BIR1* fragment was created by PCR from primers designed from WMD3 (http://wmd3.weigelworld.org). This fragment had a *Pac*I site engineered on the 5′ end. This fragment was *Pac*I digested and cloned into *Pac*I/*Eco*RV-digested pE6c-HAEpr vector. This Gateway entry vector was recombined with pGWB601 (*HAEpr*::*amiRNA BIR1*) or pGWB602 (*35S*::*HAEpr*::*amiRNA BIR1*; Nakamura et al., 2010). These constructs were transformed into *A. tumefaciens* strain GV3101 and transformed into Arabidopsis by floral dip.

To control for cross-contamination, a minimum of one representative T1 individual from each *SERK1* transgenic population was verified by using *hae-3 hsl2-3* derived cleaved-amplified polymorphic sequence (dCAPS) markers (Supplemental Table S4) and by sequencing the *SERK1* transgene across the mutation site(s) by analysis of a PCR product using *SERK1* forward primer 5′-TGGAACAACTGTTAATGAAAATCAA-3′ and pE2c reverse primer 5′-AGTCGGGCACGTCGTAGG-3′.

A PCR product from a representative T1 individual from each *HAEpr*::*YDA-YFP K429R* population was subjected to Sanger sequencing using a HAE promoter-specific primer (5′-AGGCAGAGTGCTTGTGGAGACG-3′) and a YDA-specific primer (5′-CAGGTGCCATCCAATATGGGCTC-3′). The *hae-3 hsl2-3 serk1-L326F* T1 individual also was subjected to genotyping with *serk1-L326F* dCAPS primers (Supplemental Table S4).

The strongly expressing *hae-3 hsl2-3 serk1-L326F sobir1-12* transgenic individuals were validated by genotyping with *hae-3*, *hsl2-3*, and *serk1-L326F* dCAPS markers as well as *SOBIR1* wild-type and T-DNA-specific primers.

A single T2 *hae-3 hsl2-3 + 35S::HAEpr::amiRNA BIR1* plant was validated by *hae-3* and *hsl2-3* dCAPS markers and by PCR amplifying and Sanger sequencing across the amiRNA sequence using *HAEpr* primer 5′-TTCACATGGATGTAT ACTATTGCCTCCT-3′ and amiRNA primer B 5′-GCGGATAACAATTTCACA CAGGAAACAG-3′ to ensure that it correctly aligned to the output generated by WMD3.

All constructs were created using PFU Ultra II High-Fidelity polymerase and Sanger sequence verified across the entire coding region (Agilent). All primers are listed in Supplemental Table S4.

Immunoblotting

Three whole flowers, starting with a stage 15 flower and proceeding with the next two oldest flowers, were frozen and ground in microcentrifuge tubes, resuspended in 30 μL of SDS sample buffer, and boiled for ~3 min. Ten microliters of each sample was run on an 8% (w/v) acrylamide gel, blotted to a nitrocellulose membrane, stained with Ponceau S, and imaged. Blots were blocked with 4% (w/v) BSA in phosphate-buffered saline with 0.1% Tween 20 (PBS-T) for 1 h, probed with anti-HA-horseradish peroxidase (HRP) or anti-FLAG antibody at 1:1,000 dilution for 1 h at room temperature or overnight at 4°C, respectively, and then rinsed with PBS-T four times for 5 min each (anti-HA-HRP antibody [Roche clone 3F10] and anti-FLAG antibody [Sigma M2]). HA blots were directly imaged. FLAG blots were incubated with anti-mouse HRP (1:2,500 dilution in 1% BSA in PBS-T; Cell Signaling Technologies) for 1 h at room temperature and rinsed with PBS-T four times for 5 min each. Blots were imaged by incubation with a chemiluminescent substrate (SuperSignal West Pico; Life Technologies) and imaged using a Bio-Rad ChemiDoc.

qPCR

RNA from five stage 15 receptacles was isolated using the Trizol reagent, from which cDNA was synthesized following DNase I treatment. Three or five biological replicates per reaction were performed. Tissue was harvested in balanced batches one replicate at a time to facilitate the use of a paired Student's *t* test. We used ABsolute SYBR Green Master Mix (2×; Thermo Fisher) and a Bio-Rad CFX96 thermal cycler to estimate threshold counts during the log-linear phase of amplification. Data analysis was performed in Microsoft Excel. We utilized reference gene AT5G25760 for normalization for the *hae-3 hsl2-3 serk1-L326F sobir1-12* experiment and the geometric mean of AT3G01150 and AT2G28390 for *BIR1* experiments (Czechowski et al., 2005). An eightfold serial dilution was used to calculate PCR primer efficiency and determine estimated fold change levels.

In Vitro Autophosphorylation

In vitro autophosphorylation assays were carried out exactly as described (Taylor et al., 2013). In brief, expression of MBP-SERK1 was induced by adding isopropyl-β-D-thiogalactopyranoside to rapidly growing *Escherichia coli* to a final concentration of 0.1 mM. These cultures were then allowed to grow for 4 or 6 h, after which 100 μL of liquid culture was spun down, resuspended in 100 μL of 1× SDS sample buffer, and boiled for 3 min. Ten microliters of the whole-cell lysate was then run on an 8% (w/v) acrylamide gel, after which the gel was fixed by incubation in 50% (v/v) ethanol/10% (v/v) acetic acid overnight. The gel was rehydrated by soaking in distilled, deionized water two times for 30 min and then immersed in one-third-strength Pro-Q Diamond dye for 2 h in the dark on a rotating platform (Thermo Fisher). The gel was destained in 20% (v/v) acetonitrile and 50 mM sodium acetate (pH 4) four times for 30 min each time. Then, it was soaked in distilled, deionized water twice for 10 min before imaging on a Bio-Rad ChemiDoc using the default Pro-Q Diamond settings. Finally, the gel was stained with Coomassie Blue and imaged using a Bio-Rad GelDoc. Band quantity estimates were performed using the built-in Bio-Rad software.

Statistical Analysis

For testing the timing of abscission in *serk1-1*, *serk1-L326F*, and the wild type, a Wilcoxon rank-sum test was performed on the positions of abscission using a Bonferroni correction for multiple testing. For all qPCR experiments, two genotypes were compared by performing a paired Student's *t* test on the delta-delta-Ct between the gene of interest and previously published reference gene(s) under the null hypothesis that the average of the differences was equal to 0 (Dussault and Pouliot, 2006; Yuan et al., 2006).

Accession Numbers

Sequence data from this article can be found in the GenBank/EMBL data libraries under the following accession numbers: *HAE*, NM_118991; *HSL2*, NM_125968.3; *SERK1*, NM_105841.4; *SOBIR1*, NM_128746.3; and *BIR1*, NM_124213.5.

Supplemental Data

The following supplemental materials are available.

Supplemental Figure S1. Genetic analysis of *hae hsl2* suppressor mutations.

Supplemental Figure S2. Phenotypic analysis of Col-0, *serk1-1*, and *serk1-L326F*.

Supplemental Figure S3. Analysis of the requirement of SERK1 kinase activity for *hae hsl2* suppression effect.

Supplemental Table S1. Mutant alleles of *SERK1* isolated in this study.

Supplemental Table S2. T1 transgene phenotype counts.

Supplemental Table S3. GO enrichment analysis for RNA-Seq experiments.

Supplemental Table S4. Genotyping primers used in this study.

Supplemental Data Set S1. Cuffdiff output for RNA-Seq data.

ACKNOWLEDGMENTS

We thank the skilled staff at the University of Missouri DNA Core Facility for Illumina Sequencing services. We also thank Melody Kroll (University of Missouri) for thoughtful review of the article. We thank Tsuyoshi Nakagawa (Shimane University) for providing the pGWB601/pGWB602 binary vectors containing the bar gene, which was identified by Meiji Seika Kaisha. The Gateway entry vector pE2C was obtained from Addgene. *bak1-5* was kindly provided by Antje Heese (University of Missouri). The *YDA-KI* plasmid was kindly provided by Dominique Bergmann (Stanford University).

Received October 29, 2018; accepted March 24, 2019; published April 11, 2019.

LITERATURE CITED

Adamczyk BJ, Lehti-Shiu MD, Fernandez DE (2007) The MADS domain factors AGL15 and AGL18 act redundantly as repressors of the floral transition in Arabidopsis. Plant J **50:** 1007–1019

Albrecht C, Russinova E, Hecht V, Baaijens E, de Vries S (2005) The Arabidopsis thaliana SOMATIC EMBRYOGENESIS RECEPTOR-LIKE KINASES1 and 2 control male sporogenesis. Plant Cell **17:** 3337–3349

Alonso JM, Stepanova AN, Leisse TJ, Kim CJ, Chen H, Shinn P, Stevenson DK, Zimmerman J, Barajas P, Cheuk R, et al (2003) Genome-wide insertional mutagenesis of Arabidopsis thaliana. Science **301:** 653–657

Austin RS, Vidaurre D, Stamatiou G, Breit R, Provart NJ, Bonetta D, Zhang J, Fung P, Gong Y, Wang PW, et al (2011) Next-generation mapping of Arabidopsis genes. Plant J **67:** 715–725

Baer J, Taylor I, Walker JC (2016) Disrupting ER-associated protein degradation suppresses the abscission defect of a weak hae hsl2 mutant in Arabidopsis. J Exp Bot **67:** 5473–5484

Burr CA, Leslie ME, Orlowski SK, Chen I, Wright CE, Daniels MJ, Liljegren SJ (2011) CAST AWAY, a membrane-associated receptor-like kinase, inhibits organ abscission in Arabidopsis. Plant Physiol **156:** 1837–1850

Butenko MA, Patterson SE, Grini PE, Stenvik GE, Amundsen SS, Mandal A, Aalen RB (2003) Inflorescence deficient in abscission controls floral organ abscission in Arabidopsis and identifies a novel family of putative ligands in plants. Plant Cell **15:** 2296–2307

Chen MK, Hsu WH, Lee PF, Thiruvengadam M, Chen HI, Yang CH (2011) The MADS box gene, FOREVER YOUNG FLOWER, acts as a repressor

controlling floral organ senescence and abscission in Arabidopsis. Plant J **68:** 168–185

Cho SK, Larue CT, Chevalier D, Wang H, Jinn TL, Zhang S, Walker JC (2008) Regulation of floral organ abscission in Arabidopsis thaliana. Proc Natl Acad Sci USA **105:** 15629–15634

Clough SJ, Bent AF (1998) Floral dip: A simplified method for Agrobacterium-mediated transformation of Arabidopsis thaliana. Plant J **16:** 735–743

Colcombet J, Boisson-Dernier A, Ros-Palau R, Vera CE, Schroeder JI (2005) Arabidopsis SOMATIC EMBRYOGENESIS RECEPTOR KINASES1 and 2 are essential for tapetum development and microspore maturation. Plant Cell **17:** 3350–3361

Czechowski T, Stitt M, Altmann T, Udvardi MK, Scheible WR (2005) Genome-wide identification and testing of superior reference genes for transcript normalization in Arabidopsis. Plant Physiol **139:** 5–17

Domínguez-Ferreras A, Kiss-Papp M, Jehle AK, Felix G, Chinchilla D (2015) An overdose of the Arabidopsis coreceptor BRASSINOSTEROID INSENSITIVE1-ASSOCIATED RECEPTOR KINASE1 or its ectodomain causes autoimmunity in a SUPPRESSOR OF BIR1-1-dependent manner. Plant Physiol **168:** 1106–1121

Du Z, Zhou X, Ling Y, Zhang Z, Su Z (2010) agriGO: A GO analysis toolkit for the agricultural community. Nucleic Acids Res **38:** W64–W70

Dubin MJ, Bowler C, Benvenuto G (2008) A modified Gateway cloning strategy for overexpressing tagged proteins in plants. Plant Methods **4:** 3

Dussault AA, Pouliot M (2006) Rapid and simple comparison of messenger RNA levels using real-time PCR. Biol Proced Online **8:** 1–10

Fernandez DE, Heck GR, Perry SE, Patterson SE, Bleecker AB, Fang SC (2000) The embryo MADS domain factor AGL15 acts postembryonically: Inhibition of perianth senescence and abscission via constitutive expression. Plant Cell **12:** 183–198

Gao M, Wang X, Wang D, Xu F, Ding X, Zhang Z, Bi D, Cheng YT, Chen S, Li X, et al (2009) Regulation of cell death and innate immunity by two receptor-like kinases in Arabidopsis. Cell Host Microbe **6:** 34–44

Hohmann U, Nicolet J, Moretti A, Hothorn LA, Hothorn M (2018) The SERK3 elongated allele defines a role for BIR ectodomains in brassinosteroid signalling. Nat Plants **4:** 345–351

Jaillais Y, Belkhadir Y, Balsemão-Pires E, Dangl JL, Chory J (2011) Extracellular leucine-rich repeats as a platform for receptor/coreceptor complex formation. Proc Natl Acad Sci USA **108:** 8503–8507

Jinn TL, Stone JM, Walker JC (2000) HAESA, an Arabidopsis leucine-rich repeat receptor kinase, controls floral organ abscission. Genes Dev **14:** 108–117

Kubo M, Udagawa M, Nishikubo N, Horiguchi G, Yamaguchi M, Ito J, Mimura T, Fukuda H, Demura T (2005) Transcription switches for protoxylem and metaxylem vessel formation. Genes Dev **19:** 1855–1860

Lampard GR, Lukowitz W, Ellis BE, Bergmann DC (2009) Novel and expanded roles for MAPK signaling in Arabidopsis stomatal cell fate revealed by cell type-specific manipulations. Plant Cell **21:** 3506–3517

Langmead B, Salzberg SL (2012) Fast gapped-read alignment with Bowtie 2. Nat Methods **9:** 357–359

Lee Y, Yoon TH, Lee J, Jeon SY, Lee JH, Lee MK, Chen H, Yun J, Oh SY, Wen X, et al (2018) A lignin molecular brace controls precision processing of cell walls critical for surface integrity in Arabidopsis. Cell **173:** 1468–1480.e9

Leslie ME, Lewis MW, Youn JY, Daniels MJ, Liljegren SJ (2010) The EVERSHED receptor-like kinase modulates floral organ shedding in Arabidopsis. Development **137:** 467–476

Lewis MW, Leslie ME, Fulcher EH, Darnielle L, Healy PN, Youn JY, Liljegren SJ (2010) The SERK1 receptor-like kinase regulates organ separation in Arabidopsis flowers. Plant J **62:** 817–828

Li H, Handsaker B, Wysoker A, Fennell T, Ruan J, Homer N, Marth G, Abecasis G, Durbin R (2009) The Sequence Alignment/Map format and SAMtools. Bioinformatics **25:** 2078–2079

Liljegren SJ, Leslie ME, Darnielle L, Lewis MW, Taylor SM, Luo R, Geldner N, Chory J, Randazzo PA, Yanofsky MF, et al (2009) Regulation of membrane trafficking and organ separation by the NEVERSHED ARF-GAP protein. Development **136:** 1909–1918

Meng X, Zhou J, Tang J, Li B, de Oliveira MVV, Chai J, He P, Shan L (2016) Ligand-induced receptor-like kinase complex regulates floral organ abscission in Arabidopsis. Cell Rep **14:** 1330–1338

Nakamura S, Mano S, Tanaka Y, Ohnishi M, Nakamori C, Araki M, Niwa T, Nishimura M, Kaminaka H, Nakagawa T, et al (2010) Gateway binary vectors with the bialaphos resistance gene, bar, as a selection marker for plant transformation. Biosci Biotechnol Biochem **74:** 1315–1319

Niederhuth CE, Cho SK, Seitz K, Walker JC (2013a) Letting go is never easy: Abscission and receptor-like protein kinases. J Integr Plant Biol **55:** 1251–1263

Niederhuth CE, Patharkar OR, Walker JC (2013b) Transcriptional profiling of the Arabidopsis abscission mutant hae hsl2 by RNA-Seq. BMC Genomics **14:** 37

Ogawa M, Kay P, Wilson S, Swain SM (2009) ARABIDOPSIS DEHISCENCE ZONE POLYGALACTURONASE1 (ADPG1), ADPG2, and QUARTET2 are polygalacturonases required for cell separation during reproductive development in Arabidopsis. Plant Cell **21:** 216–233

Patharkar OR, Walker JC (2015) Floral organ abscission is regulated by a positive feedback loop. Proc Natl Acad Sci USA **112:** 2906–2911

Patharkar OR, Walker JC (2016) Core mechanisms regulating developmentally timed and environmentally triggered abscission. Plant Physiol **172:** 510–520

Patharkar OR, Gassmann W, Walker JC (2017) Leaf shedding as an antibacterial defense in Arabidopsis cauline leaves. PLoS Genet **13:** e1007132

Patterson SE (2001) Cutting loose: Abscission and dehiscence in Arabidopsis. Plant Physiol **126:** 494–500

Santiago J, Henzler C, Hothorn M (2013) Molecular mechanism for plant steroid receptor activation by somatic embryogenesis co-receptor kinases. Science **341:** 889–892

Santiago J, Brandt B, Wildhagen M, Hohmann U, Hothorn LA, Butenko MA, Hothorn M (2016) Mechanistic insight into a peptide hormone signaling complex mediating floral organ abscission. eLife **5:** e15075

Schardon K, Hohl M, Graff L, Pfannstiel J, Schulze W, Stintzi A, Schaller A (2016) Precursor processing for plant peptide hormone maturation by subtilisin-like serine proteinases. Science **354:** 1594–1597

Stenvik GE, Tandstad NM, Guo Y, Shi CL, Kristiansen W, Holmgren A, Clark SE, Aalen RB, Butenko MA (2008) The EPIP peptide of INFLORESCENCE DEFICIENT IN ABSCISSION is sufficient to induce abscission in Arabidopsis through the receptor-like kinases HAESA and HAESA-LIKE2. Plant Cell **20:** 1805–1817

Taylor I, Walker JC (2018) Transcriptomic evidence for distinct mechanisms underlying abscission deficiency in the Arabidopsis mutants haesa/haesa-like 2 and nevershed. BMC Res Notes **11:** 754

Taylor I, Seitz K, Bennewitz S, Walker JC (2013) A simple in vitro method to measure autophosphorylation of protein kinases. Plant Methods **9:** 22

Trapnell C, Roberts A, Goff L, Pertea G, Kim D, Kelley DR, Pimentel H, Salzberg SL, Rinn JL, Pachter L (2012) Differential gene and transcript expression analysis of RNA-seq experiments with TopHat and Cufflinks. Nat Protoc **7:** 562–578

Weigel D, Ahn JH, Blázquez MA, Borevitz JO, Christensen SK, Fankhauser C, Ferrándiz C, Kardailsky I, Malancharuvil EJ, Neff MM, et al (2000) Activation tagging in Arabidopsis. Plant Physiol **122:** 1003–1013

Yan L, Ma Y, Liu D, Wei X, Sun Y, Chen X, Zhao H, Zhou J, Wang Z, Shui W, et al (2012) Structural basis for the impact of phosphorylation on the activation of plant receptor-like kinase BAK1. Cell Res **22:** 1304–1308

Yuan JS, Reed A, Chen F, Stewart CN Jr (2006) Statistical analysis of real-time PCR data. BMC Bioinformatics **7:** 85